Short communication

Copper nitrate hydrate as novel high capacity anode material for lithium-ion batteries
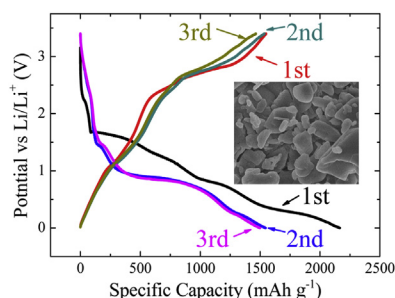
CrossMark

Kaiqiang Wu, Dongjie Wang, Lianyi Shao, Miao Shui, Rui Ma, Mengmeng Lao, Nengbing Long, Yuanlong Ren, Jie Shu*

Faculty of Materials Science and Chemical Engineering, Ningbo University, Ningbo 315211, Zhejiang Province, People's Republic of China

HIGHLIGHTS

- For the first time, $Cu(NO_3)_2 \cdot xH_2O$ is studied as a novel lithium storage anode material.
- $Cu(NO_3)_2 \cdot xH_2O$ exhibits an initial discharge capacity of about 2200 mAh g^{-1}.
- $Cu(NO_3)_2 \cdot xH_2O$ obtained at 160 °C delivers a reversible capacity of 597.6 mAh g^{-1} after 30 cycles.

GRAPHICAL ABSTRACT

ABSTRACT

For the first time, $Cu(NO_3)_2 \cdot xH_2O$ ($x \leq 2.5$) is investigated as a new lithium storage anode material for lithium-ion batteries. The impressive characteristic of $Cu(NO_3)_2 \cdot xH_2O$($x \leq 2.5$)/Li cell is the high initial discharge capacity reaching to around 2200 mAh g^{-1}. To make a comparison, $Cu(NO_3)_2 \cdot 2.5H_2O$ electrodes are used as raw materials and heat-treated at 80, 120 and 160 °C. Among all the three samples, $Cu(NO_3)_2 \cdot xH_2O$ ($x < 2.5$) obtained at 160 °C shows the highest reversible capacity of 597.6 mAh g^{-1} and the best cycling stability after 30 cycles. The difference in electrochemical behaviors is attributed to the variation of surface morphology, crystal water and particles size after heat-treatment at different temperatures. Besides, the thermal reaction results also show that $Cu(NO_3)_2 \cdot xH_2O$ ($x < 2.5$) obtained at 160 °C has the highest thermal stability among all the three samples after repeated cycles. The present findings can provide the fact that $Cu(NO_3)_2 \cdot xH_2O$ (≤ 2.5) may be a promising anode material for lithium-ion batteries.

© 2013 Elsevier B.V. All rights reserved.

1. Introduction

It is well known that transition metal oxides express the advantages of higher specific capacity, better electrochemical stability and more excellent cycle retention than conventional carbonaceous materials [1–3]. Among different kinds of transition metal oxides, CuO attracted more attentions because of its high theoretic specific capacity of 670 mAh g^{-1}. Moreover, it is generally accepted that different morphologies of CuO, such as nanoflower [2], hollow dandelion-like spheres [4] and leaf-shaped [5], show different electrochemical performances as anodes in lithium-ion batteries. However, those transition metal oxides suffer from severe drawbacks, such as poor electronic conductivity and huge polarization in lithium-ion batteries, which are the main hindrances to their commercial use. Due to these limitations, it seems necessary to turn the efforts towards complex transition metal oxides [6–8] or synthesis of transition metal oxides/carbon composites [9–11] to improve the electrochemical properties.

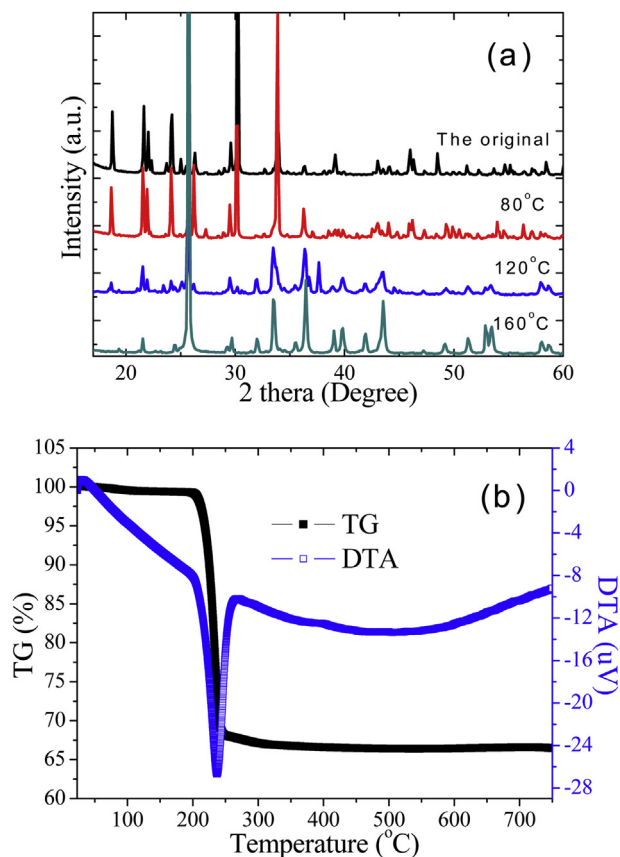**Fig. 1.** (a) XRD patterns of $Cu(NO_3)_2 \cdot xH_2O$ ($x \leq 2.5$) samples obtained at different heat-treatment temperatures and (b) TG-DTA curves of $Cu(NO_3)_2 \cdot 2.5H_2O$ in argon.

Most recently, many transition metal nitrides have been widely studied as anode materials due to their high reversibility, large reversible capacity and satisfactory stability [12–14]. As reported [12], Cu_3N exhibited good cycle life and excellent rate capability as a candidate anode material. Meanwhile, the reaction mechanism of Ge_3N_4 [13] with lithium was investigated as well. It exhibits high capacity of 500 mAh g^{-1}. Moreover, ternary lithium transition metal nitrides, such as Li_3FeN_2 [15] and Li_7MnN_4 [16], have been introduced in the last two decades, which show good cycle stability and high specific capacity. However, those ternary lithium transition metal nitrides undergo the drawback of moisture sensitivity before being treated as electrode materials in lithium-ion batteries.

Till now, no report about nitrates as lithium storage materials has been reported in the past decades. In the present work, copper nitrate hydrate is studied as a novel high capacity anode material for lithium-ion batteries, and its electrochemical properties and physical characterizations are examined.

2. Experimental

$Cu(NO_3)_2 \cdot 2.5H_2O$ (Aladdin Chemistry) was purchased with analytical grade and used as received without further purification. The slurry for working electrode was composed of $Cu(NO_3)_2 \cdot 2.5H_2O$, carbon black, and polyvinylidene fluoride as a binder with a composition of 4:1:1 in *N*-methyl pyrrolidinone solvent. Then the slurry was coated on Cu-foil collector as working electrode and treat-treated at 80, 120 and 160 °C in vacuum for 12 h.
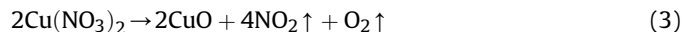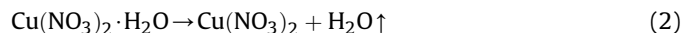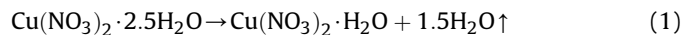
The electrochemical cells were composed of copper nitrate hydrate electrode as working electrode, metallic lithium foils as reference and counter electrodes, 1 M LiPF$_6$ dissolved in ethylene

carbonate–dimethyl carbonate (1:1 in volume) as electrolyte, and Whatman glass fiber as separator. The simulated cells were assembled in an argon-filled glove box. The patterns for micro-structure were measured by Bruker AXS D8 Focus X-ray diffraction (XRD) instrument. The surface morphologies were observed by Hitachi S3400 scanning electron microscopy (SEM). Electro-chemical characteristics of the cells were recorded by multi-channel Land battery test system. Electrochemical impedance spectroscopy (EIS) analysis was carried out by CHI 660D electro-chemical workstation with the frequency range of $10^5–10^{-2}$ Hz. Thermogravimetric (TG) and differential thermal analysis (DTA) behaviors of the original and lithiated samples were investigated by a Seiko TG/DTA 6300 apparatus with a heating rate of 10 °C min^{-1} in the temperature range from 23 to 800 °C under argon atmosphere.

3. Results and discussion

Fig. 1a shows the XRD patterns of copper nitrate hydrate heat-treated at different temperatures. As seen from Fig. 1a, it is clear that the seven strongest peaks at 18.82, 21.56, 21.99, 24.18, 29.64, 30.29 and 33.90° are in good agreement with the (110), (−211), (211), (−204), (114), (−404) and (314) lines in the JCPDS card No. 75-1493 representing the compound of $Cu(NO_3)_2 \cdot 2.5H_2O$. The cell parameters of $Cu(NO_3)_2 \cdot 2.5H_2O$ are $a = 16.45$ Å, $b = 4.941$ Å, $c = 15.96$ Å and $\beta = 93.750°$ with a space group of $12/a$. Fig. 1a also shows the XRD patterns of copper nitrate hydrate obtained at 80, 120 and 160 °C, which are similar to the original pattern before heat-treatment, except for the change of relative intensity. No impurity, such as CuO and Cu_3N, can be observed in Fig. 1a.

The typical TG-DTA curves of commercial $Cu(NO_3)_2 \cdot 2.5H_2O$ are characterized in the argon atmosphere as shown in Fig. 1b. The obtained profile clearly indicates that the decomposition process of $Cu(NO_3)_2 \cdot 2.5H_2O$ proceeds in several steps. It can be observed that a slight weight loss of 0.7% appears between 23 and 200 °C, which is contributed to the evaporation of absorbed water and the partial loss of crystallized water. An abrupt weight loss of 31.3% occurs between 200 and 250 °C from the TG curves, assigning to the total loss of crystallized water and the following decomposition of $Cu(NO_3)_2$ powders into CuO and gaseous products. These decomposition steps are in accordance with those suggested by I.V. Morozov [17] and can be expressed by following equations:

$$Cu(NO_3)_2 \cdot 2.5H_2O \rightarrow Cu(NO_3)_2 \cdot H_2O + 1.5H_2O\uparrow \qquad (1)$$

$$Cu(NO_3)_2 \cdot H_2O \rightarrow Cu(NO_3)_2 + H_2O\uparrow \qquad (2)$$

$$2Cu(NO_3)_2 \rightarrow 2CuO + 4NO_2\uparrow + O_2\uparrow \qquad (3)$$

Based on the above decomposition process and XRD results, it is clear that $Cu(NO_3)_2 \cdot 2.5H_2O$ may lose different amounts of crystallized water after heat-treatment at different temperatures (80, 120 and 160 °C). Therefore, the sample heat-treated at different temperatures should be defined as $Cu(NO_3)_2 \cdot 2.5H_2O$ for 80 °C and $Cu(NO_3)_2 \cdot xH_2O$ ($x < 2.5$) for 120 and 160 °C.

Fig. 2a–f compares the surface morphologies of $Cu(NO_3)_2 \cdot xH_2O$ ($x \leq 2.5$) samples obtained at 80, 120 and 160 °C. It is clear that distinct difference in the practice size appears due to different heat-treatment temperatures. After a heat-treatment at 80 °C, the sample shows the aggregation of many rod-like particles into bigger secondary particles. The size of rod-like particles ranges from 2.0 to 4.0 μm as observed in Fig. 2a and b. Furthermore, a layer of film-like substance is covering on the surface of samples which makes the formation of larger bulk secondary particles. The